# Fluorination of polymers by means of He-CF₄ fed

# atmospheric pressure glow dielectric barrier discharges

Fiorenza Fanelli,* Francesco Fracassi, Riccardo d'Agostino

Dipartimento di Chimica, Università degli Studi di Bari–IMIP CNR, via  Orabona 4,

70126 Bari, Italy

Fax: +39 0805443405; E-mail: fiorenzafanelli@chimica.uniba.it

## Keywords

## Abstract

Helium-tetrafluoromethane (He-CF₄) fed Glow Dielectric Barrier Discharges (GDBDs) were used to fluorinate polypropylene (PP) and polyethyleneterephtalate (PET). The effect of various process parameters on polymers surface composition and morphology as well as on their wettability was investigated inside the GDBD existence domain. An

extensive surface fluorination of treated polymers due to the grafting of F atoms and $CF_x$ radicals was observed. The increase of $CF_4$ concentration in the feed, of treatment duration, and of excitation frequency resulted in an increase of the fluorination degree corresponding to F/C ratios as high as 1.18 and 1.22 for PP and PET, respectively. The emission spectra of GDBDs fed by helium in mixture with $CF_4$, $CHF_3$, $C_2F_6$ and $C_3F_8$ were compared.

## Introduction

Low pressure glow discharges fed with fluorocarbons have been widely and successfully employed for the etching of inorganic and organic materials, for the deposition of fluoropolymers as well as for the treatment of synthetic and natural polymers. Many rigorous investigations allowed to clarify the role of the reactive gas, of its F/C ratio, of additives (i.e. oxygen or hydrogen), and the effect of several process parameters such as input power, pressure, discharge regime (i.e. continuous and modulated) and of other variables. The careful correlation between surface properties and gas phase composition allowed to gain important insights into the plasma-surface interaction.

Tetrafluoromethane fed plasmas, which were traditionally used in microelectronics for dry etching applications, have been also extensively utilized for the treatment of several polymers [1-9]. These plasmas are populated by F atoms, $CF_x$ ($1 \leq x \leq 3$) fragments and ions produced by the fragmentation of the reactive gas [10-13]. It has been demonstrated that if the F/C ratio of the monomer is high, as for $CF_4$, also the $[F]/[CF_x]$

ratio in the plasma is high, plasma polymerization is inhibited while the grafting of fluorinated functionalities on polymer surfaces can be achieved [1-9].

For instance, M. Strobel et al. [1] studied the fluorination of polyolefins by means of low pressure $CF_4$ plasma and obtained, after a 30 s treatment, a F/C ratio of 0.94 and 1.02 for polyethylene and polypropylene, respectively. The treated surfaces were characterized by the presence of different fluorinated functionalities such as C-CF, CF, $CF_2$ and $CF_3$ groups. Fluorine atoms were considered the main responsible of the fluorination process, even though the contribution of $CF_x$ radicals could not be excluded. The proposed fluorination mechanism was composed by an initiating step of hydrogen abstraction from the polyolefinic chain by fluorine atom to form HF and an alkyl radical and a subsequent reaction of this radical with fluorine resulting in the formation of C-F bonds on the polymer surface. As also discussed by Hopkins et al. [6], the abstraction/fluorination mechanism is thermodinamically favoured for the higher values of the H-F and C-F bond energies (5.9 eV and 5.0 eV, respectively) with respect to the C-H bond in polyolefins (3-4 eV). $CF_x$ radicals were supposed to be responsible for the formation of highly fluorinated components ($CF_3$ groups, in particular). This was confirmed by Strobel et al. [1] which observed that a polymer surface treated in $SF_6$ plasmas, in which $CF_x$ radicals are not present, is characterized by negligible amount of $CF_3$ functionalities, thus the presence of $CF_3$ groups on the polymer surfaces treated in $CF_4$ plasmas was considered an indication of the $CF_x$ radicals involvement in the overall fluorination process.

F. Poincin-Epaillard et al. [3] highlighted the dependence of fluorination extent on the chemical composition of the untreated polymer; e.g. polyesters fluorination was weaker than that of polyolefins. Similar results were also reported by Hopkins et al. [7], in fact

after treatment in $CF_4$ plasma the F/C ratio for polypropylene and polyethyleneterephtalate was 1.1 and 0.72, respectively.

The fluorination of polyethylene (PE) films with $CF_4$ fed plasmas as a function of frequency and electrode configuration was studied by Y. Khairallah et al. [2]. Treatments were performed at 13.56 MHz with a symmetric reactor and at a 70 kHz and 13.56 MHz with a highly asymmetric (corona configuration) apparatus. With corona configuration, for treatment shorter than 1 s, only CO and CF groups were grafted (hydrophilic character of the treated polymer). The increase of treatment duration favoured the grafting of more fluorinated groups, such as $CF_2$ and $CF_3$ (up to the F/C ratio of 1.5 at 13.56 MHz), and the hydrophobic character of the treated surfaces. On the other hand with symmetric configuration and 13.56 MHz, the F/C ratio did not exceed 1.2 also for long treatment times.

In recent years, efforts have focused on the utilization of atmospheric pressure dielectric barrier discharges (DBDs), both in filamentary and glow regime, in fields traditionally dominated by low pressure plasmas. S. Kanazawa and co-workers [14-15] studied the fluorination of PET in Atmospheric Pressure Glow Discharges (APGDs) fed with He-$CF_4$. With a $CF_4$/He ratio in the feed of 0.048 and 300 s of treatment, they obtained F/C and O/C ratios approximately of 1.2 and 0.2, respectively, along with an increase of the water contact angle with respect to the untreated polymer.

I. Vinogradov and A. Lunk [16-18] performed a spectroscopic investigation of filamentary DBDs fed with Ar and several fluorocarbons. In $CF_4$ containing plasma a broad emission in the range 450-750 nm and an intense band in the UV region ascribed to $CF_3$ were reported. The intensity of the first band and of $CF_2$ emissions increased with F/C ratio of the fluorocarbon molecule contained in the feed gas.

In spite of the important preliminary published results, only few works have been published on the utilization of DBDs for the grafting of fluorine-containing functionalities on polymer surfaces and therefore detailed and systematic investigations are needed. These investigations should be focused to achieve an extensive grafting of fluorinated groups onto the polymeric surfaces with a reliable process control, and to the clarification of process mechanism by coupling both surface and plasma investigations.

The present work concerns the fluorination of polypropylene and polyethyleneterephtalate surfaces by He-$CF_4$ fed glow dielectric barrier discharges (GDBDs) are reported. The effect of several process parameters on polymers surface composition and morphology, as well as on their wettability, was evaluated under the experimental conditions where the discharge is in the glow regime. The two polymers utilized as substrates, namely a saturated polyolefin (PP) and an aromatic polyester (PET), allowed to investigate the influence of the polymer chemical structure on the fluorination process. An extensive spectroscopic investigation of the plasma phase was also carried out by Optical Emission Spectroscopy.

## Experimental

The experimental apparatus consists of a parallel plate electrode system (5 mm interelectrodic distance) contained in an airthight Plexiglas box; each electrode (3 × 3 $cm^2$ area) is covered by a 0.6 mm thick $Al_2O_3$ plate (CoorsTek, 96% purity) [19, 20]. The plasma was generated by applying an AC high voltage (< 3 $kV_{p-p}$) in the frequency

range 20 - 30 kHz by means of an AC high voltage (HV) power supply, composed by a variable frequency generator (TTi TG215), a linear amplifier (Outline PA4006) and a high voltage transformer (Montoux, 10 $kV_{rms}$).

The electrical characterization of the discharge was performed with a digital oscilloscope (Tektronix TDS2014). Applied voltage ($V_a$) was measured by means of a high voltage probe (Tektronix P6015A, 75 MHz bandwidth, 1000 attenuation factor), while the current was evaluated by measuring, with a voltage probe (Tektronix P2200, 200 MHz bandwidth, 10 attenuation factor), the voltage drop across a 50 $\Omega$ resistor ($R_m$) connected in series with the ground electrode. Signals were visualized on a digital oscilloscope (Tektronix TDS2014, 100 MHz bandwidth and 2 GS/s sample rate) and transmitted to a PC by a communication module (TDS-CMA Tektronix). The average power density dissipated by the discharge was calculated as the integral over one cycle of the product of the applied voltage and the current divided by the period and the electrode area. The average current density of the discharge was calculated as the mean peak-to-peak current over three periods divided by the electrode area. The average power density and the average current density were the average value of five different experiments.

The discharge was fed with He-$CF_4$ mixtures (Airliquide, Helium C and R14Tetrafluoromethane 100 %). The gas flow rates were controlled by MKS electronic mass flow controllers, while system pressure was monitored by a MKS 122 baratron. Feed gas was introduced in the interelectrodic zone through a slit and pumped through a second slit positioned on the opposite side, therefore a longitudinal gas injection was realized.

Optical emission spectroscopy investigation was performed in the UV-Vis region (200 – 900 nm) using an Optical Multichannel Analyser (OMA) equipped with a monochromator (0.300 m focal length imaging monochromator SP-300i ACTON, 1200 g/mm grating) and a CCD intensified detector (SpectruMM$^{TM}$ 100B, Princeton Instruments). The spectra were collected with an entrance slit of 50 μm that allowed to obtain a nominal bandwidth of 0.168 nm. In order to exclude the presence of second order signals, the spectra in the wavelength range 450 - 900 nm were registered using a long pass filter (cut-off wavelength of 450 nm). OES of DBDs fed by helium and various fluorocarbons, such as $CHF_3$ (Airliquide, 99.9+% purity), $C_2F_6$ (Zentek, 99+% purity) and $C_3F_8$ (Airliquide, 99+% purity), was also performed.

X-ray Photoelectron Spectroscopy (XPS) analyses were carried out by means of a Theta Probe spectrometer (Thermo Electron Corporation) equipped with a non-monochromatic Al $K_\alpha$ radiation (1486.6 eV). Survey (0-1100 eV) and high resolution (HR) spectra (C1s, F1s, O1s, N1s) were recorded at a pass energy of 150 eV and 50 eV, respectively. Spectra were acquired with a take-off angle (TOA) of 37°. Angle resolved XPS analyses (ARXPS) were also performed in order to investigate the evolution of the chemical composition of the polymers as a function of the take-off angle (22°, 32°, 42°, 52°, 62°), i.e. as a function of sampling depth; lower take-off angles correspond to shorter sampling depths.

The F/C and O/C XPS ratios were derived from high resolution spectra, considering the area of the C 1s, F 1s and O 1s peaks. For the quantitative analysis, the highest estimated error was of 1 %. For the treated polymeric surfaces a nitrogen uptake lower than 1% has been detected. The C1s signals for the hydrocarbon component (285.0 eV) and for the aromatic component (284.7 eV) were used as internal standard for charging

correction for PP and PET, respectively. [21]. Best fitting of C1s and O1s high resolution spectra was performed using Advantage Data Spectrum Processing software (Thermo Electron Corporation). The full-width at half maximum (FWHM) of each line-shape was allowed to vary between 1.3 – 1.7 for untreated PET and between 1.7 – 2.2 eV for plasma treated PP and PET substrates. The FWHM of peaks belonging to the same high-resolution spectrum was usually allowed to differ up to 0.2 eV. Details on the curve fit components are reported in the next section. Unless otherwise specified the atomic concentration ratios and high resolution spectra refer to a TOA of 37°.

Surface wettability was evaluated by static and dynamic water contact angle (WCA) measurements, using a Ramé-Hart manual goniometer (model A-100). Contact angles were measured on both sides of five drops of double distilled water for each sample and the average value was calculated with a maximum uncertainty of ± 3°. The average value of WCA in the region 10 - 20 mm from the gas entrance inside the discharge area was considered [19-20]. Advancing and receding contact angles (AWCA and RWCA) were measured according to the sessile drop method.

Scanning electron microscopy (SEM) analyses were carried out by a digital microscope EVO 40XVP (Zeiss) to probe surface topography before and after plasma treatment. The specimens were sputter-coated with a 60 nm thick gold thin film.

In order to compare the results obtained under different experimental conditions, XPS analyses, WCA measurements and morphological investigations were carried out considering the region 10–20 mm from the gas entrance inside the discharge area [19-20].

The effect of several process parameters, such as feed composition, frequency (f), and treatment duration ($t_{tr}$), was investigated inside the GDBD operational window.

Biaxially oriented polypropylene (Goodfellow, 13 μm thickness) and biaxially oriented polyethyleneterephtalate (Goodfellow, 125 μm thickness) were used as substrates. Before plasma treatment polymers were cleaned with ethanol (J.T. Baker, Absolute ethanol, purity of 99.9 %) and dried at room temperature.

Fluorination process were preformed using a helium flow rate ($\phi_{He}$) of 4 slm and a $CF_4$ volume concentration ranging between 0.05 % and 0.30 %. The excitation frequency ($f$) was changed in the range 20 - 30 kHz, and the input voltage ($V_a$) was kept constant at 2.8 $kV_{p-p}$. The treatment duration was varied from 10 s to 600 s.

The experimental conditions utilized in this study are summarized in Table 1.

## Results and discussion

**Electrical characterization of the discharge**

The electrical characterization of the discharge showed that, in the frequency range 20-30 kHz and at a peak-to-peak voltage lower than 3 kV, a glow DBD can be obtained for a $CF_4$ concentration in helium up to 0.3 %; for higher concentrations a filamentary discharge occurs. As reported in figure 1a, in agreement with published data [22], the He-$CF_4$ fed GDBD is characterized by a periodical discharge current signal composed by only one peak per half-cycle. The amplitude of the current peak increases with $CF_4$ concentration in the feed gas; at 25 kHz and 2.8 $kV_{p-p}$ the average current density increases from (10.0 ± 0.5) mA·cm$^{-2}$ for a pure He GDBD, to (14.0 ± 1) mA·cm$^{-2}$ and (16.0 ± 1) mA·cm$^{-2}$ for a [$CF_4$] of 0.05 % and 0.3 %, respectively. For concentrations

higher than 0.3 %, even though the current is still formed by only one peak per half-cycle, the signal is not periodical since the intensity changes in each period (Figure 1b) and probably microdischarges formation occurs. Thus, 0.3 % of $CF_4$ in helium can be considered as the threshold concentration under which the typical features of a GDBD can be obtained, beyond this threshold, a decrease of the discharge current density occurs.

At 2.8 $kV_{p-p}$ and 0.2 % of $CF_4$ in He, the increase of the frequency from 20 kHz to 30 kHz, resulted in an increase of the average discharge current density from $(9.0 \pm 0.5)$ $mA \cdot cm^{-2}$ to $(18.0 \pm 0.9)$ $mA \cdot cm^{-2}$ as well as in a growth of the average power density from $(0.30 \pm 0.02)$ $W \cdot cm^{-2}$ to $(0.40 \pm 0.04)$ $W \cdot cm^{-2}$.


**Plasma fluorination of polymers**

Figure 2 shows the trends of the XPS F/C and O/C ratios and of the static WCA values for polypropylene and polyethyleneterephtalate treated for 120 s at 25 kHz and 2.8 $kV_{p-p}$ as a function of the $CF_4$ concentration in He-$CF_4$ fed GDBDs. Plasma treatment induces an intense fluorination of the polymer surface which increases with $CF_4$ concentration in the feed gas. The average power density does not appreciably change with $[CF_4]$ and it is equal to $(0.34 \pm 0.04)$ $W \cdot cm^{-2}$.

For polypropylene the F/C ratio varies from 1.06 to 1.18 when $[CF_4]$ passes from 0.05 to 0.3 %. Some oxygen is also present on the treated surface due to uptake of $O_2$ and/or $H_2O$ contaminants in the plasma and/or to post-treatment oxidation after atmospheric exposure. By increasing $[CF_4]$, an increase of hydrophobic character was detected by static and dynamic WCA measurements. Static WCA increases from 90° for the untreated polymer to 113° at 0.3% $[CF_4]$ while advancing and receding WCAs increase

from 101° to 125° and from 83° to 95°, respectively. The WCA hysteresis (difference between the advancing and the receding WCA values) is approximately 30° and does not change as a function of the [CF$_4$] in the feed.

An analogous increase of the XPS F/C ratio was observed for treated PET as a function of the [CF$_4$], even though the fluorination degree was lower with respect to PP. Plasma treatment also reduces the XPS O/C ratio of PET from 0.37 for the untreated polymer to approximately 0.25, whatever the fluorocarbon concentration in the feed. Of course, as previously discussed for PP, a certain fraction of bonded oxygen could be due to contaminants uptake and/or post-treatment reactions with atmospheric oxygen and water vapour. The static WCA increases from 76° for the untreated polymer to 109° at 0.3% [CF$_4$], while the advancing and receding WCAs vary from 80° to 118° and from 60° to 91°.

Further information on the chemical characteristics of treated surfaces can be obtained by comparing the high resolution XPS C1s spectra before and after plasma treatment in He-0.3%CF$_4$ fed GDBD. As expected (Figure 3), virgin PP is characterized by a symmetric C1s peak centred at 285.0 eV due to aliphatic carbon [21] while the treated surface displays high BE components ascribed to fluorinated functionalities. The best fitting of the signal was performed using, in addition to the C-C peak at 285.0 eV, the five new components reported in table 2. Respect to published data [1, 3] the overall CF$_3$ percent (i.e. CF$_3$ and O$\underline{C}$F$_3$%) is quite high (14.4 %). If the CF$_4$ concentration in the feed is reduced down to 0.05 % a slight decrease of fluorine containing components is registered.

O1s is centred at 535.2 eV, the peak is asymmetric, degraded towards lower binding energies, to indicate the presence of oxygen atoms directly bounded to highly

fluorinated groups, e.g. OCF$_3$. The formation of OCF$_3$ could probably support the incorporation of oxygen in the reaction chamber during the plasma process because it is unlikely that OCF$_3$ forms from oxidation and successive restructuring of treated surface after air exposure. On the other hand trifluoromethoxy functionalities are stabilized by the negative hyperconiugation effect of CF$_3$ group which acts as $\pi$-acceptor and stabilizes the ether bond by interacting with the oxygen lone pairs [23-24].

Figure 4 reports the XPS C1s and O1s regions of PET before and after 120 seconds of plasma treatment ([CF$_4$] = 0.3%). As expected, the C1s peak of the untreated polymer consists of C-C (285.0 ± 0.2 eV), C-O (286.6 ± 0.2 eV) and O=C-O (289.0 ± 0.2 eV) components and of a weak shake-up peak at 291.5 eV due to the aromatic rings of the polymer structure [21]. After the plasma treatment, the C1s signal is fitted with six peaks (table 2).  In this case, CF$_3$O groups could form both for grafting at the polyester carboxylic functionalities and/or for oxygen uptake during the plasma process. The presence of CF$_3$O on treated surface is also confirmed by O1s signal which, in addition to the O=C and O-C contribution of pristine surface, shows a new peak  at higher binding energy (535.4 eV) due to  oxygen atoms bound to highly fluorinated groups. As for PP, also with  PET the overall CF$_3$ percentage is quite high (16.5%). By decreasing the [CF$_4$] concentration in the feed down to 0,05 a slight decrease  of CF and CF$_2$ occurs, while OCF$_3$ concentration remains about 6 %.

The effect of treatment duration was studied for both polymers in the time range 10 – 600 s. During the first 120 seconds,  the XPS concentration of atomic fluorine  increases steeply  up to 50% and 45 % for PP and PET, respectively and then  remains almost constant. Treatment duration affects also oxygen concentration  which  shows  the

strongest reduction within the first 30 s. In particular with increasing the treatment duration from 10 s to 30 s the oxygen atomic concentration decreases from 10 % to 5 % for PP and from 16 % to 12 % for PET; a similar trend was detected for $OCF_3$. Any significant variation of contact angle was evidenced.

Angle resolved XPS analyses showed that for all treatment durations, fluorine incorporation occurs mainly on the topmost layers of the polymers since, in both cases, the F/C ratio increase by decreasing the take-off angle, i.e. by reducing the sampling depth. While for PP oxygen concentration is constant within the thickness examined, in the case of PET oxygen concentration increases with sampling depth.

SEM observation, carried out before and after plasma treatment, showed that the surface topography of the original polymers is not appreciably affected also after 600 s of treatment.

When the excitation frequency is increased from 20 to 30 kHz at 2.8 $kV_{p-p}$, 120 s of treatment, and $[CF_4]$ of 0.2 %, the F/C ratio passes from 0.8 to 1.1 for PP and from 0.55 to 1.2 for PET; the oxygen content decreases and the fluorination degree is higher for PET than for PP.

The higher fluorination with excitation frequency could be due to a more intense activation of the reactive gas, which increases with the number of discharge current pulses per unit of time and with the average discharge current density and, as a consequence, with the increase of the average power density from $(0.30 \pm 0.02)$ $W \cdot cm^{-2}$ to $(0.40 \pm 0.04)$ $W \cdot cm^{-2}$. As evident in figure 5, for both polymers frequency increase results in a higher percent of $CF_2$ and $CF_3$ and in a lower quantity of $OCF_3$.

**Gas phase investigation**

The He-$CF_4$ fed GDBD was characterized by intense emissions from helium, atomic fluorine and $CF_2$ bands in the spectral range 240 – 350 nm ($A^1B_1 - X^1A_1$ system) [25, 26]. Several emissions related to impurities, such as nitrogen, oxygen and water [25, 26] as well as $CO^+$ (first negative system) and $CO_2^+$ (Fox-Duffendack and Barker system) emissions were also detected [26], indicating the occurrence of oxidation reactions in the gas phase and/or at the polymer surface. The emission of nitrogen- and oxygen-containing species could be related to the oxygen and nitrogen uptake at the polymeric surfaces. The emission of the $B^2\Delta - X^2\Pi$ CF system (197 – 220 nm), often detected in low pressure fluorocarbon plasmas, was never observed [26-29], while between 220 and 250 nm, the presence of emissions probably due to the $A^2\Delta - X^2\Pi$ CF system was detected [26, 27] even though due to the spectral interference of $CF_2$ and $CO^+$ the identification is not confident.

Figure 6 reports the typical emission spectra in the wavelength ranges 220 – 380 nm and 500 – 750 nm for a He-0.2%$CF_4$ GDBD at 25 kHz. The continuum at approximately 620 nm (figure 6b) is assigned to $CF_3$ radicals [30] which undergo a transition from an electronically excited state to a repulsive lower state yielding $CF_2$ and F. This emission is responsible of the pale yellow colour of the plasma [30].

Between 220 and 380 nm two continua, centred at approximately 240 and 290 nm, respectively, are present. The identification of these emissions is complicated and not univocal. According to d'Agostino et al. [10-12], the continuum at 290 nm could be related to $CF_2^+$ since it should originate from the $4b_2$ state (16.40 eV) of $CF_2^+$ which undergoes a transition to the $6a_1$ state (12.27 eV), which is highly C-F antibonding and weakly F-F bonding, yielding $C^+$ and two F atoms or a $F_2$ molecule. The emission at

240 nm does not seem due to the so called UV emission of $CF_3$ (transition from an electronically excited state to the ground state of $CF_3$ radical) since it is structureless and does not present the expected rotovibrational features [17, 31-34].

A possible interpretation of the both continua derives from published data on UV emission produced by electron and ion impact of $CF_4$ which report the appearance of a wide continuum emission between 200 and 300 nm consisting of two maxima at 230 nm and 290 nm, respectively. The emissions could be related to the formation of $CF_4^+$ ions in the $\widetilde{C}\,^2T_2$ state which undergoes transitions to the ground ($\widetilde{A}\,^2T_2$) and to the fist excited ($\widetilde{X}\,^2T_1$) states which are responsible of the structureless maxima at 230 nm and 290 nm, respectively [35-37]. Continua are observed since the $\widetilde{A}$ and the $\widetilde{X}$ states of the $CF_4^+$ ion are unstable and dissociates to $CF_3^+$ and F. These two continua have been detected only for $CF_4$ and not for other fluoromethanes such us $CF_3H$, $CF_3Cl$, $CF_2Cl_2$, $CFCl_3$ [38].

Another hypothesis, by U. Muller et al. [39] considers the overall emissions from 220 to 380 nm originated by excited $CF_3^+$ ions formed either from directly electron collision of $CF_4$ or resulting from the rapid dissociation of an initially formed $CF_4^+$ ion in an excited state. Then the excited $CF_3^+$ ion undergoes a transition responsible of the continuum emissions to a lower unstable state of $CF_3^+$ which dissociates perhaps into $CF_2^+$ + F and/or $CF^+$ and two F atoms (or $F_2$).


In order to attempt the identification of the two continua centred at 240 and 290 nm, the optical emission of GDBDs fed with different fluorocarbons, e.g. $CF_4$, $CHF_3$, $C_2F_6$ and $C_3F_8$ in helium are compared in Figure 7. It can be observed that while the continuum at 290 nm is always detected, that at 240 nm appears only with $CF_4$. In agreement with

references [35-38], therefore, the continuum at 240 nm can be related to species present in a significant amount only in $CF_4$ fed GDBDs i.e. $CF_4$ or $CF_4^+$.

In $CHF_3$, $C_2F_6$ and $C_3F_8$ fed GDBDs, the fact that the continuum at 290 nm appears even if that at 240 nm is not present, allows to exclude the it is correlated to $CF_4$ or $CF_4^+$ but it is reasonable to assume that it is comes from $CF_2^+$, as supposed by d'Agostino et al. [10-13]. Of course, in He-$CF_4$ GDBDs to the continuum at 290 nm could be due to $CF_2^+$ and related to $CF_4$ or $CF_4^+$.

Figure 7 shows that by increasing the $CF_4$ concentration in the feed from 0.01 to 0.3 % the continua at 240 and 290 nm increase (along with that at 620 nm), while the intensity of the superimposed $CF_2$ emission band decreases. A decrease of the intensity of emissions of F and He atoms as well as those of impurities is detected.

All the plasma emissions increase with the excitation frequency of the GDBD.

## Conclusion

In this work polypropylene and polyethyleneterephtatalate were treated in He-$CF_4$ fed GDBDs. The effect of various process parameters on polymer surface composition, morphology and wettability was investigated inside the GDBD existence domain adequately evaluated by electrical measurements. An extensive fluorination of the topmost layers of treated polymers was observed. The presence of highly fluorinated components suggests that grafting involves also $CF_x$ radicals.

As expected, the increase of $CF_4$ concentration in the feed (0.05 - 0.3 %), of treatment duration (10 – 120 s), and of the excitation frequency (20 - 30 kHz), result in a higher

fluorination degree and hydrophobicity. F/C ratios as high as 1.18 and 1.22 were obtained for PP and PET, respectively.

The fluorination extent depends on the chemical composition of the polymers, in fact polypropylene, a saturated polyolefin, generally shows a higher F/C than polyethylenthereftalate, an aromatic polyester. Only for long treatment time (600 s) or high frequency (30 kHz)   the PET fluorination degree is equal or higher than for PP.

Polypropylene shows an oxygen uptake due to $O_2$ and $H_2O$ contaminations in the reactor chamber and/or to post-treatment oxidation after atmospheric exposure. The presence of $OCF_3$ groups, which are unlikely formed from oxidation after atmospheric exposure and successive restructuring, supports the hypothesis that oxygen is incorporated during the plasma process. Trifluoromethoxy functionalities were also observed for PET and they can originate from grafting and/or for oxygen uptake.

The optical emission spectroscopic investigation of the plasma phase allowed to compare emission spectra of GDBDs fed by $CF_4$, $CHF_3$, $C_2F_6$ and $C_3F_8$ in He. It was observed that the  continuum emissions centered at 240 nm is related to species present only in $CF_4$ containing GDBDs while that centered at 290 nm could be ascribed to $CF_2^+$ and related to species present only in $CF_4$ DBDs.

## Acknowledgments

# References

[1]   M. Strobel, S. Corn, C. S. Lyons, G. A. Korba, *J. Polym. Sci.: Part A: Polym. Chem,* **1987**, *25*, 1295.

[2]   Y. Khairallah, F. Arefi, J. Amouroux, *Thin Solid Films* **1994**, *241*, 295.

[3]   F. Poincin-Epaillard, B. Pomepui, J.-C. Brosse, *J. Polym. Sci.: Part A: Polym. Chem.* **1993**, *31*, 2671.

[4]   W. Wang, F. Poincin-Epaillard, J.-C. Brosse, D. Ausserre, *Plasmas Polym.* **1996**, *1*, 65.

[5]   C.-M. Chan, T.-M. Ko, H. Hiroaka, *Surf. Sci. Rep.* **1996**, *24*, 1.

[6]   J. Hopkins, J. P. S. Babyal, *J. Phys. Chem.* **1995**, *99*, 4261.

[7]   J. Hopkins, R. D. Boyd, J. P. S. Babyal, *J. Phys. Chem.* **1996**, *100*, 6755.

[8]   H. T. Sahin, S. Minolache, R. A. Young, F. Denes, *Cellulose* **2002**, *9*, 171.

[9]   C.-H. Wen, M.-J. Chuang, G.-H. Hsiue, *Appl. Polym. Sci.* **2006**, *252*, 3799.

[10]  R. d'Agostino, F. Cramarossa, S. De Benedictis, G. Ferraro, *J. Appl. Phys.* **1981**, *52*, 1259.

[11]  R. d'Agostino, F. Cramarossa, S. De Benedictis, *Plasma Chem. Plasma Process.* **1982**, *2(3)*, 213.

[12]  R. d'Agostino, F. Cramarossa, F. Fracassi, F. Illuzzi, in *Plasma Deposition, Treatment and Etching of Polymers*, R. d'Agostino ed., Academic Press, New York, 95, 1990.

[13]  R. d'Agostino, in *Plasma Processing of Polymers*, R. d'Agostino, P. Favia and F. Fracassi eds., Kluwer Acad. Publ., NATO ASI Series, E: Appl. Sci., 346, 3, 1997.

[14] S. Kanazawa, M. Kogoma, S. Okazaki, T. Moriwaki, *Nucl. Instr. Meth. Phys. Res.* **1989**, *R37/38*, 842.

[15] T. Yokoyama, M. Kogoma, S. Kanazawa, T. Moriwaki, S. Okazaki, *J. Phys. D: Appl. Phys.* **1990**, *23*, 1125.

[16] I. P. Vinogradov, A. Dinkelmann, A. Lunk, *Surf. Coat. Technol.* **2003**, *174-175*, 509.

[17] I. P. Vinogradov, A. Dinkelmann, A. Lunk, *J. Phys. D: Appl. Phys*. **2004**, *37*, 3000.

[18] I. P. Vinogradov, A. Lunk, *Plasma Process. Polym.* **2005**, *2*, 201.

[19] F. Fanelli, F. Fracassi, R. d'Agostino, *Plasma Process. Polym.* **2005**, *2*, 688.

[20] F. Fanelli, R. d'Agostino, F. Fracassi, *Plasma Process. Polym.* **2007**, *4*, 797.

[21] G. Beamson, D. Briggs, *High Resolution XPS of Organic Polymers*, J. Wiley & Sons, Chichester, 1992.

[22] F. Massines, G. Gouda, J. Phys D.: Appl. Phys. **31**, 3411 (1998).

[23] I. Fleming, *Frontier Orbitals and Organic Chemical Reactions*, Wiley Interscience (J. Wiley & Sons), New York, 1976.

[24] H. Fukaya, T. Ono, T. Abe, *J. Phys. Chem. A* **2001**, *105*, 7401.

[25] A. R. Striganov, N. S. Sventiskii, *Tables of Spectral Lines of Neutral and Ionized Atoms*, IFI/Plenum, New York-Washington, 1968.

[26] R. W. B. Pearse, A. G. Gaydon, *The Identification of Molecular Spectra*, 4th ed., Chapman and Hall, London, 1976.

[27] D. S. King, P. K. Schenck, J. C. Stephenson, *J. Molec. Spectroscopy* **1979**, *78*, 1.

[28] J. Bretagne, F. Epaillard, A. Ricard, *J. Polym. Sci. A: Polym. Chem.* **1992**, *30*, 323.

[29] P. Venkateswarlu, *Phys. Rev.* **1950**, *77(5)*, 676.

[30] D. Flamm, *J. Appl. Phys.* **1980**, *78*, 11.

[31] M. Suto, N. Washida, *J. Chem. Phys.* **1983**, *78*, 1007.

[32] M. Suto, N. Washida, *J. Chem. Phys.* **1983**, *78*, 1012.

[33] M. Suto, N. Washida, H. Akimoto, M. Nakamura, *J. Chem. Phys.* **1983**, *78*, 1019.

[34] C. Larrieu, M. Chaillet, A. Dargelos, *J. Chem. Phys.* **1992**, *96*, 5.

[35] F. M. Aarts, *Chem. Phys. Lett.* **1985**, *114(1)*, 114.

[36] J. F. M. Aarts, S. M. Mason, R. P. Tuckett, *Mol. Phys.***1987**, *60*, 761.

[37] I. R. Lambert, S. M. Mason, R. P. Tuckett, *J. Chem. Phys.* **1988**, *89*, 2683.

[38] H. A. Van Sprang, H. H. Borgersma, F. J. De Heer, *Chem. Phys.* **1978**, *35*, 51.

[39] U. Muller, T Bubel, G. Schulz, A. Sevilla, *Z. Phys. D-Atoms, Mol. Clust.* **1992**, *24*, 131, 1992.

**Table 1** Experimental conditions for polymer fluorination in He – CF$_4$ GDBDs.

| $f$ (kHz) | $V_a$ (kV$_{p-p}$) | $\phi_{He}$ (sccm) | $\phi_{CF_4}$ (sccm) | $[CF_4]$ (%) | $t_{tr}$ (s) |
|-----------|-------------------|-------------------|---------------------|--------------|-------------|
| 25 | 2.8 | 4000 | 2 – 12 | 0.05 – 0.30 | 120 |
| 25 | 2.8 | 4000 | 8 | 0.20 | 10 – 600 |
| 20-30 | 2.8 | 4000 | 8 | 0.20 | 120 |

**Table 2** Components utilized for curve fit of XPS C1s of treated PP and PET [21].

| PP | | | | | | |
|---|---|---|---|---|---|---|
| C1s component | C-C | CO/<u>C</u>-CF | CF | CF$_2$ | CF$_3$ | OCF$_3$ |
| BE (eV) | 285.0 ± 0.2 | 287.1 ± 0.3 | 289.4 ± 0.2 | 291.5 ± 0.2 | 293.5 ± 0.2 | 295.3 ± 0.2 |

| PET | | | | | | |
|---|---|---|---|---|---|---|
| C1s component | C-C | C-O/<u>C</u>-CF | O=C-O /CF | CF$_2$ | CF$_3$ | OCF$_3$ |
| BE (eV) | 284.7 ± 0.2 | 286.4 ± 0.3 | 288.7 ± 0.2 | 290.8 ± 0.2 | 292.8 ± 0.2 | 294.4 ± 0.2 |
| O1s component | O=C | O-C | O-CF$_x$ | | | |
| BE (eV) | 531.7 ± 0.2 | 533.3 ± 0.2 | 535.1 ± 0.2 | | | |

**Figure captions**

Figure 1. Applied voltage and measured current at 25 kHz and 2.8 $kV_{p-p}$ for a He-0.3%$CF_4$ fed GDBD (a) and a He-0.5% $CF_4$ fed FDBD (b).

Figure 2. XPS F/C and O/C ratios and static WCA values for PP and PET as a function of [$CF_4$] in the feed (f = 25 kHz, $t_{tr}$ = 120 s).

Figure 3. (a) High resolution XPS C1s spectrum of untreated PP and (b) best fit of C 1s spectrum of polypropylene treated with He-0.3%$CF_4$ fed GDBD (f = 25 kHz, $t_{tr}$ = 120 s). Experimental data are reported as grey line, while the peaks originated by curve fitting are black.

Figure 4. Best fit of high resolution XPS C 1s and O1s spectra of PET before (a) and after the treatment with a He-0.3%$CF_4$ fed GDBD (f = 25 kHz, $t_{tr}$ = 120 s) (b). Experimental data are reported as grey line, while the peaks originated by curve fitting are black.

Figure 5. Curve fit of XPS C1s spectra of PP and PET treated with a He-$CF_4$ fed GDBD at 20 kHz and 30 kHz ([$CF_4$] = 0.2 %, $t_{tr}$ = 120 s).

Figure 6. Emission spectra of He-$CF_4$ fed GDBD (f = 25 kHz, [$CF_4$] = 0.2 %) in the wavelengths range 200-380 nm (a) and 500-750 nm (b).

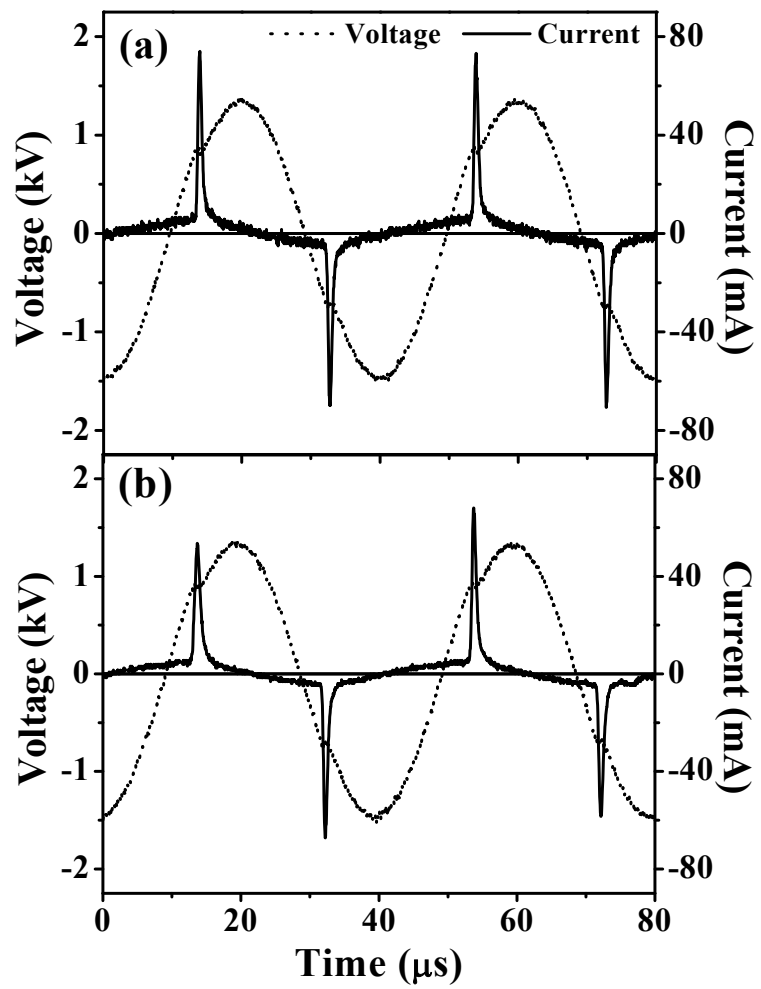Figure 7. Emission spectra of GDBDs at 25 kHz fed with He-$CF_4$ ([$CF_4$] = 0.01 %, 0.2 %), He-$CHF_3$ ([$CHF_3$] = 0.01 %, 0.2 %), He-$C_2F_6$ ([$C_2F_6$] = 0.01 %), He-$C_3F_8$ ([$C_3F_8$] = 0.01 %).
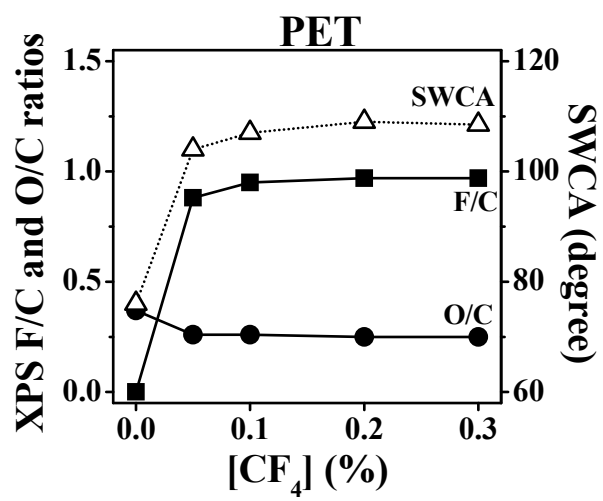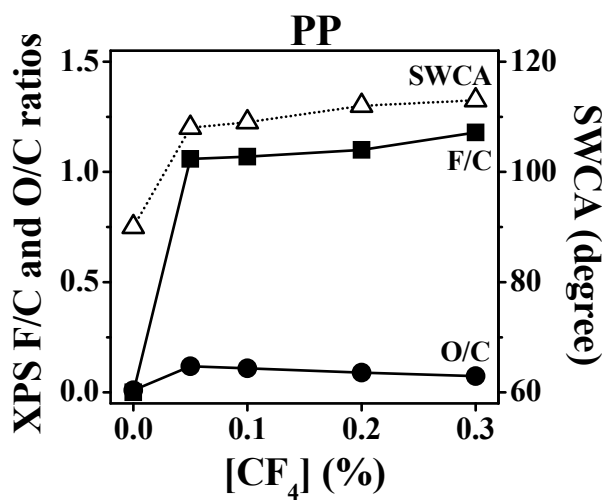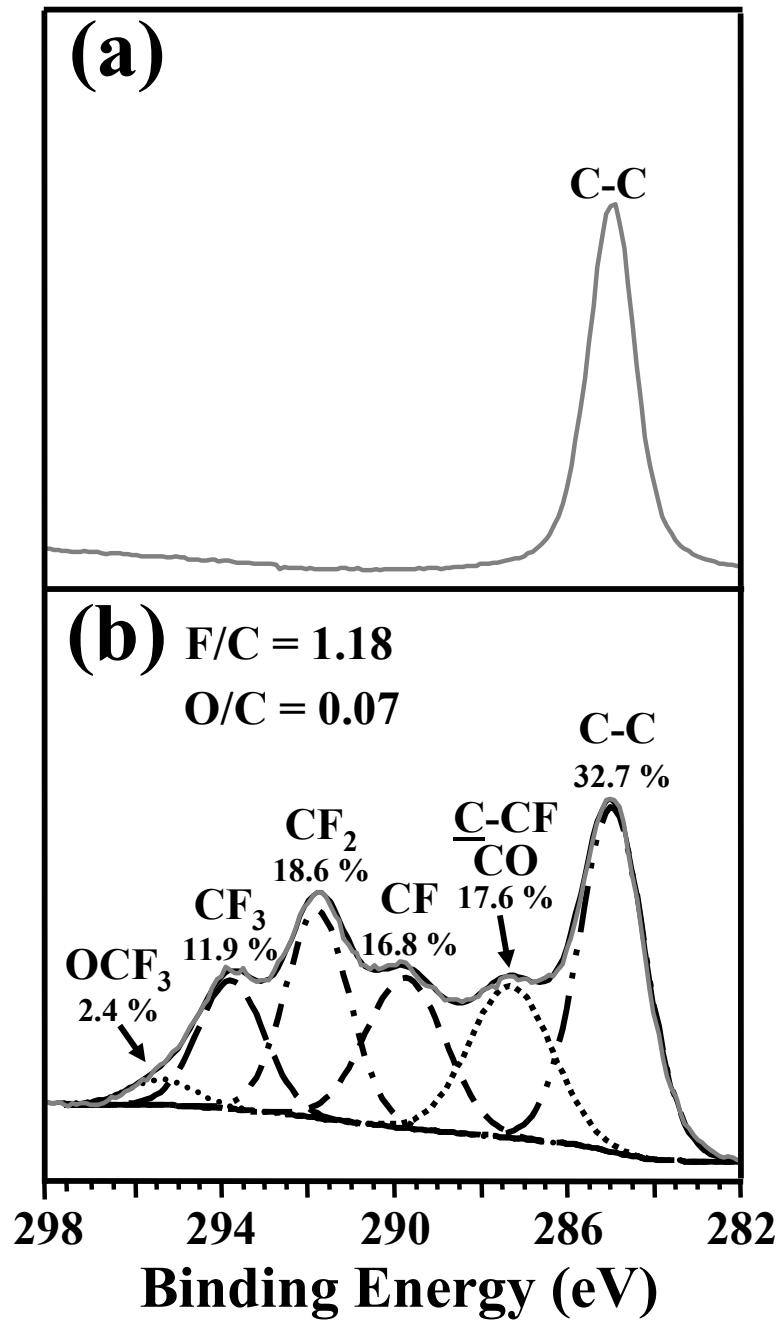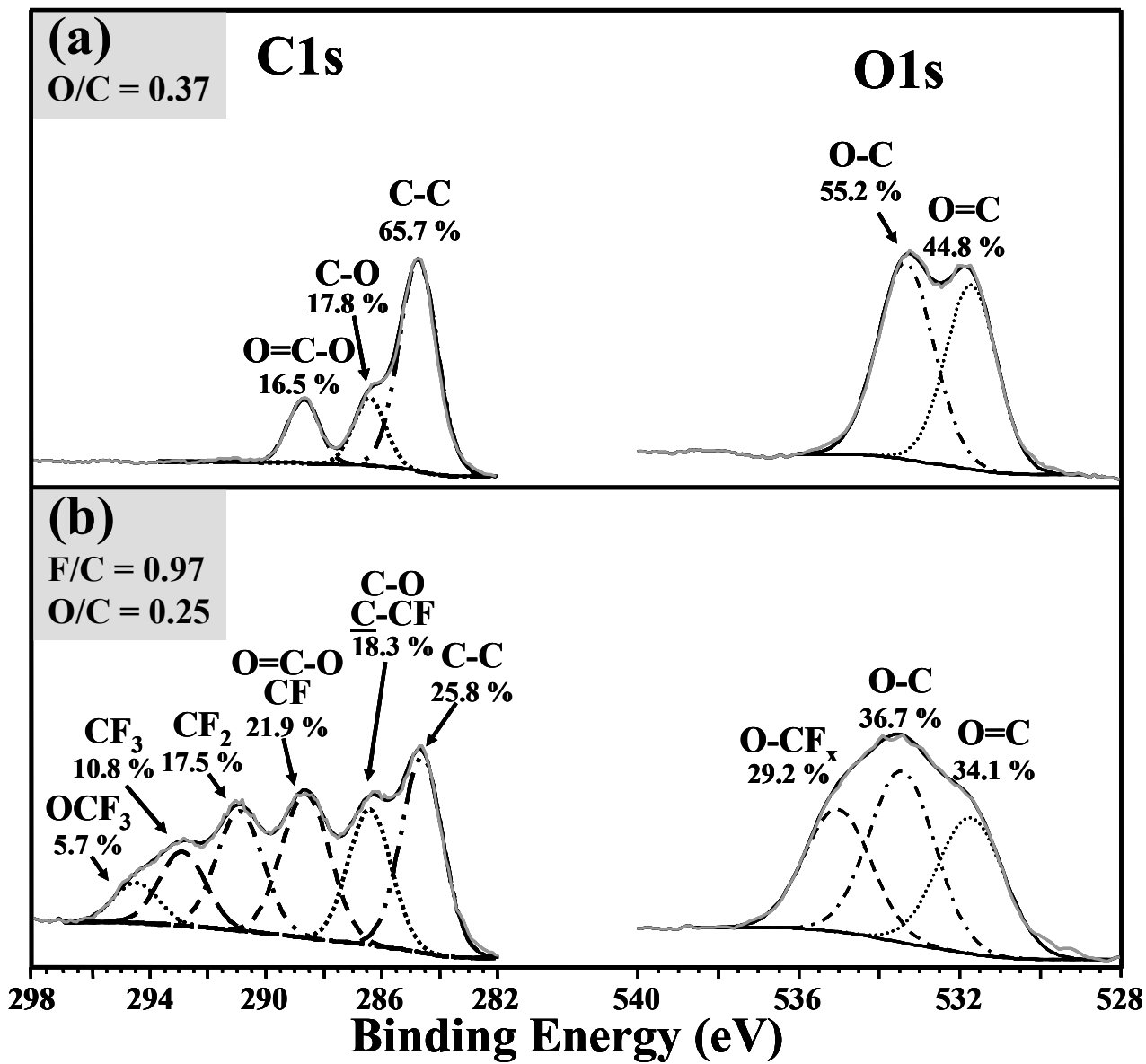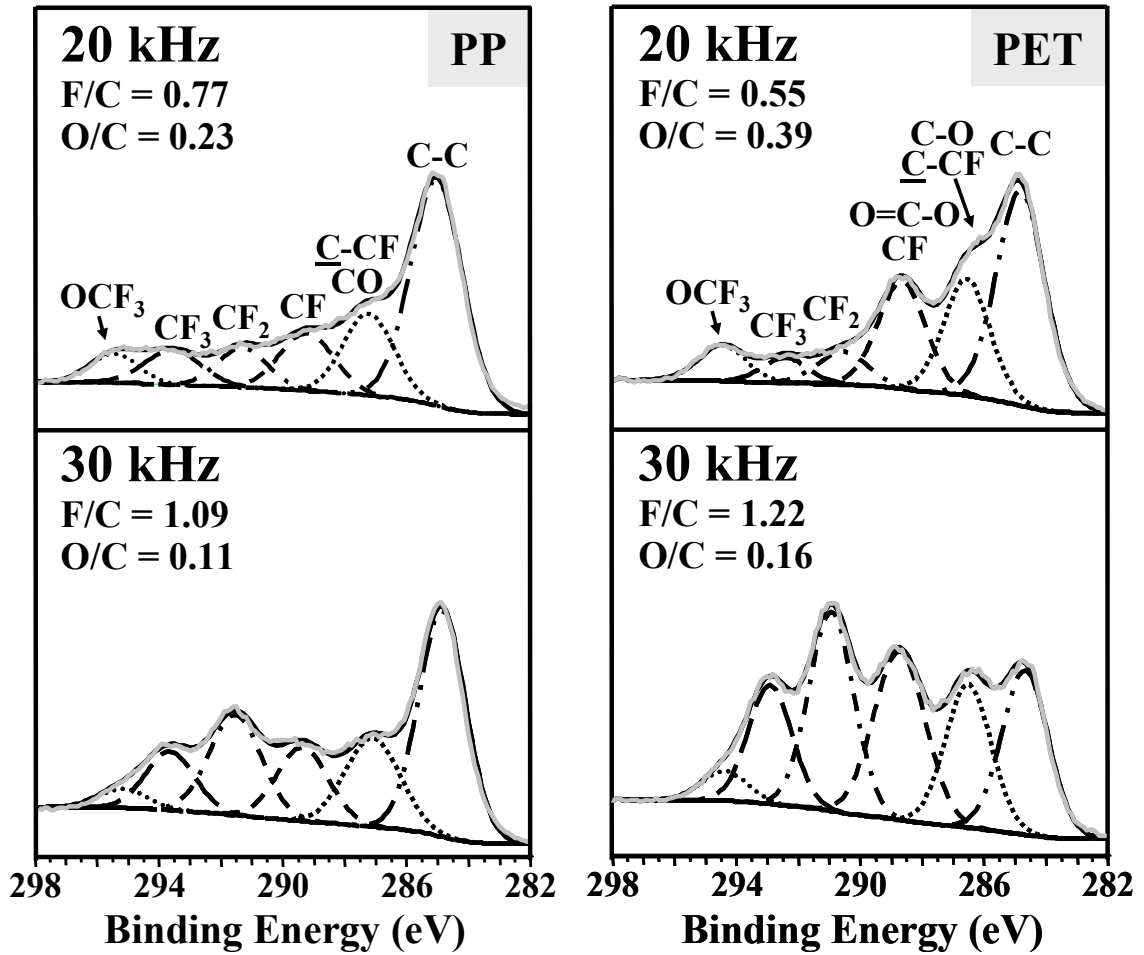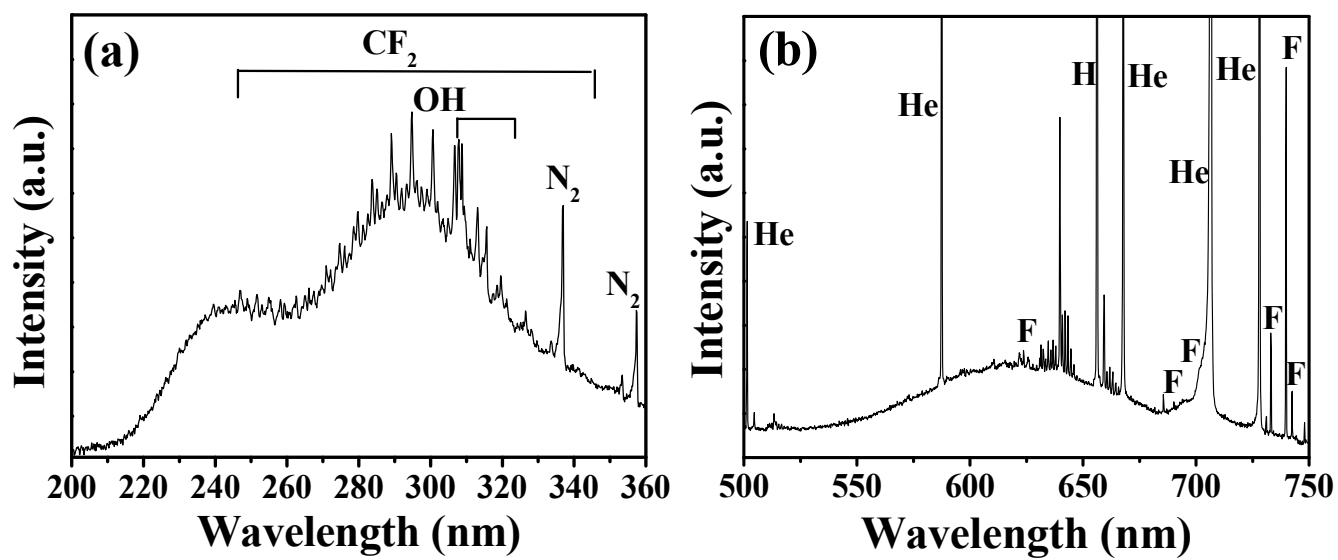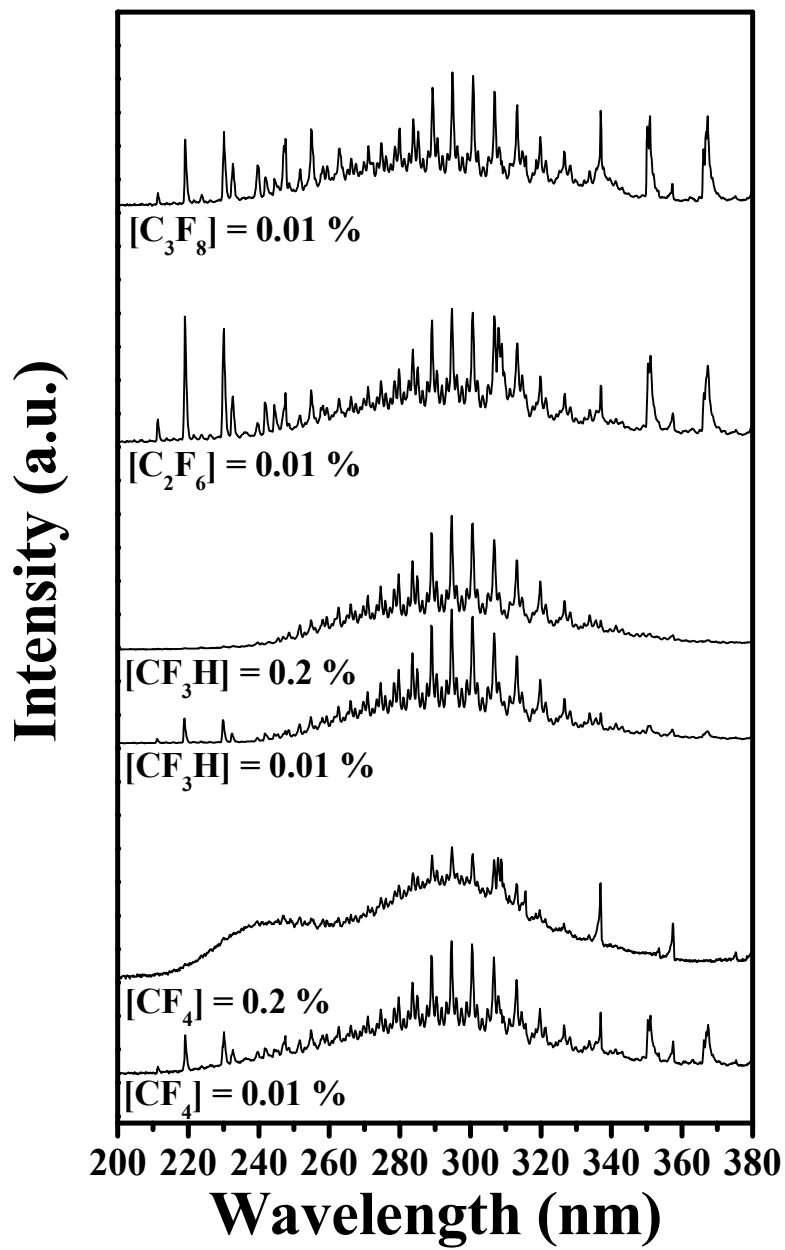
Figure 1

23

Figure 2

Figure 3

Figure 4

Figure 5

Figure 6

Figure 7